

High-resolution spectroscopy of the R Coronae Borealis Star V Coronae Australis[★]

N. Kameswara Rao¹ & David L. Lambert²

¹*Indian Institute of Astrophysics, Bangalore 560034, India*

²*The W.J. McDonald Observatory, The University of Texas, Austin, TX 78712-1083, USA*

Accepted Received ; in original form

ABSTRACT

Optical high-resolution spectra of the R Coronae Borealis star V CrA at light maximum and during minimum light are discussed. Abundance analysis confirms previous results showing that V CrA has the composition of the small subclass of R Coronae Borealis (RCB) stars known as ‘minority’ RCBs, i.e., the Si/Fe and S/Fe ratios are 100 times their solar values. A notable novel result for RCBs is the detection of the 1-0 Swan system $^{12}\text{C}^{13}\text{C}$ bandhead indicating that ^{13}C is abundant: spectrum synthesis shows that $^{12}\text{C}/^{13}\text{C}$ is about 3 to 4. Absorption line profiles are variable at maximum light with some lines showing evidence of splitting by about 10 km s^{-1} . A spectrum obtained as the star was recovering from a deep minimum shows the presence of cool C_2 molecules with a rotational temperature of about 1200K, a temperature suggestive of gas in which carbon is condensing into soot. The presence of rapidly outflowing gas is shown by blue-shifted absorption components of the Na I D and K I 7698 Å resonance lines.

Key words: Star: individual: R CrB: variables: circumstellar matter :other

1 INTRODUCTION

R Coronae Borealis stars (here, RCBs) are a rare class of peculiar variable stars. The two defining characteristics of RCBs are (i) a propensity to fade at unpredictable times by up to about 8 magnitudes as a result of obscuration by clouds of soot, and (ii) a supergiant-like atmosphere that is very H-deficient and He-rich. The subject of this paper, V Coronae Australis (V CrA) is even a peculiar member of this class of peculiar stars. It is a ‘minority’ R CrB. The distinction between majority and minority members was made first by Lambert & Rao (1994) on the basis of an abundance analysis of warm RCBs. The minority RCBs are quite severely deficient in iron relative to the majority RCBs and to the Sun but some elements, particularly Si and S, have near-solar abundances in the minority (and majority) RCBs. This combination results in some very unusual abundance ratios, for example, the Si/Fe and S/Fe ratios of minority

RCBs are approximately 100 times the solar ratios. V CrA also seems to be an especially lively producer of dust (Feast et al. 1997). The realization that V CrA is an unusual RCB led us to occasional spectroscopic monitoring of its optical spectrum.

The current paper discusses high-resolution spectroscopic observations obtained on seven occasions between 1989 and 2003 when the star was either at or near maximum light or in decline by 3 to 5 magnitudes. A suitable spectrum at maximum light is subjected here to an abundance analysis. The previous analysis (Asplund et al. 2000) was based on a spectrum obtained during a shallow light minimum. This spectrum may have been contaminated by phenomena expected at minimum light (i.e., some lines may have been filled in partially by emission). In addition, our new spectra cover a broader bandpass at higher resolution and signal-to-noise ratio than the earlier spectrum. Other spectra show for the first time for V CrA line splitting indicative of the presence of an atmospheric shock. Spectra taken at minimum light are discussed in the context of our detailed studies of 1995-96 and 2003 minima of R CrB (Rao et al 1999; Rao, Lambert & Shetrone 2006).

[★] Based on observations obtained with (1) The Blanco 4m Telescope at the Cerro Tololo Inter-American Observatory, which is operated by AURA, Inc., under contract to the National Science Foundation of USA, and (2) The Harlan J. Smith Telescope of the W.J. McDonald Observatory of the University of Texas at Austin.

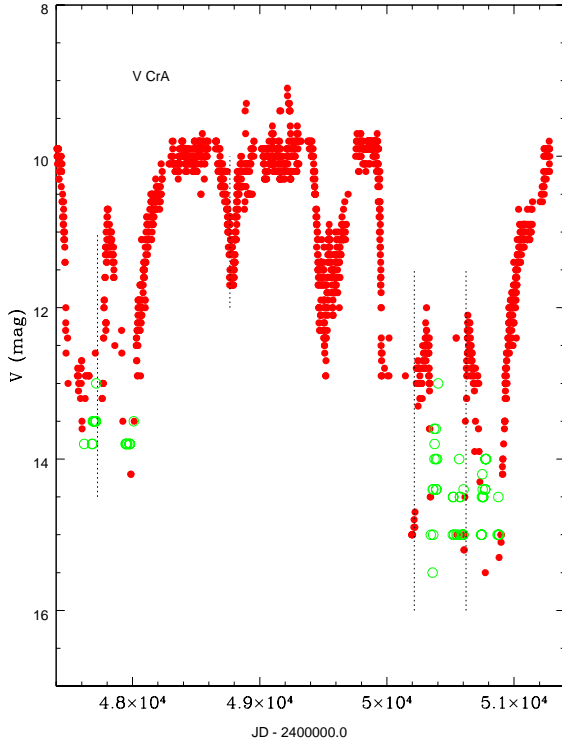


Figure 1. The visual (red dots) light curve of V CrA showing the several light minima during 1988–1998 period. Dates on which four spectroscopic observations were obtained are indicated by a dashed line (also see Table 1). Upper limits to the brightness are shown by green unfilled circles. The observations are from the AAVSO database.

2 OBSERVATIONS

Observations (Table 1) of V CrA were obtained on four occasions with the cross-dispersed echelle spectrograph of the Harlan J. Smith 2.7m reflector at the W.J. McDonald observatory (Tull et al. 1995). The spectral resolving power, $R = \lambda/d\lambda$, employed was 60000. The spectrum covers 3900 to 10000 Å with gaps beyond about 5600 Å where the echelle orders were incompletely captured on the Tektronix 2048 x 2048 CCD. On three of the four occasions, V CrA was at maximum light (Figure 2).

Spectroscopic observations (Table 1) were also obtained on three occasions with the Cassegrain echelle spectrometer on the 4m Blanco reflector at CTIO. The resolving power employed was close to 30000 for the 1989 and 1992 spectra and about 40000 for the 1996 spectrum. The spectral coverage was 5420 Å to 6840 Å during 1989, 5480 Å to 7090 Å in 1992, and 5750 Å to 8150 Å in 1996. On all the three occasions, the star was below its maximum brightness (Figure 1).

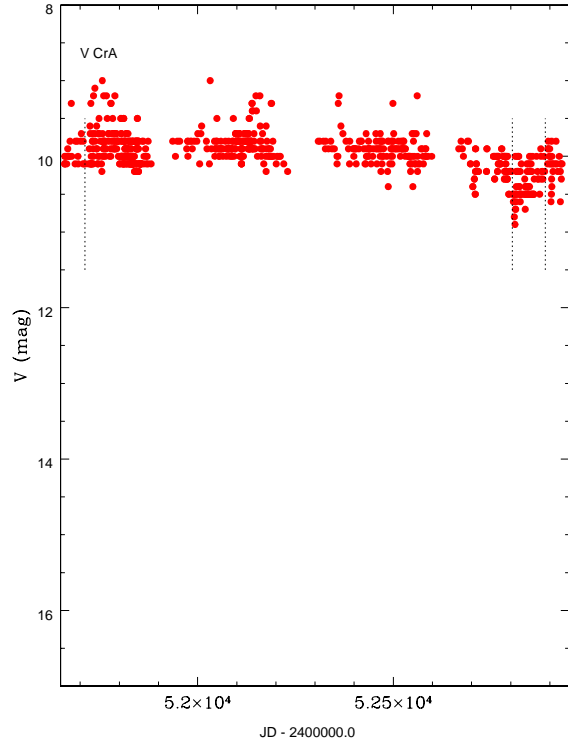


Figure 2. The visual (red dots) light curve of V CrA during 2000 - 2003 period. Dates on which three spectroscopic observations (at maximum light) obtained are indicated by dashed lines (also see Table 1). The observations are from the AAVSO database.

3 V CRA'S SPECTRUM AT MAXIMUM LIGHT

3.1 General features

Spectra at maximum light are dominated by lines of C I, as expected of an RCB star, and by lines of Si I and S I in addition to the many lines seen in spectra of normal F-G supergiants. Even at maximum light, the star shows changes in absorption line profiles, particularly a variable doubling of some lines, a phenomenon attributable to pulsations. Percy et al. (2004) found a photometric period of 106 days with a range in V of 0.3 magnitudes during 1987-88. Lawson & Cottrell (1997) found periods ranging from 57 days to 108 days from photometry during 1986–1989. However, their radial velocity measurements showed a variable velocity from 14 measurements spanning 13.3 km s^{-1} with a period of 75 or 125 days. Another notable feature is shown by the strongest lines: the profiles of the O I triplet lines at 7774 Å, for example, show extended blue wings indicative of a high velocity wind. The spectra include the C₂ Swan system bands. Unique to V CrA among RCBs observed to date is the clear presence of the 1-0 Swan band at 4744 Å from the $^{12}\text{C}^{13}\text{C}$ molecule.

3.2 Radial velocity and line doubling

The 2003 September 6 spectrum shows photospheric absorption lines with symmetrical profiles. This spectrum is taken

Table 1. Spectroscopic Observations of V CrA.

Date (UT)	Julian Date (2400000+)	Magnitude V (or vis)	Telescope	Observer ^a	Comment
1989 July 16	47723.755	13	CTIO 4.0m	DLL	recovery
1992 May 22	48764.838	10.9	CTIO 4.0m	DLL NKR	decline
1996 May 11	50214.856	14.8	CTIO 4.0m	SB	recovery
1997 June 22	50621.820	13	McDonald 2.7m	DLL NKR	recovery
2000 June 16	51711.779	10.0	McDonald 2.7m	DY	maximum
2003 June 13	52803.876	10.3	McDonald 2.7m	BER NKR	maximum
2003 Sept. 6	52888.605	10.1	McDonald 2.7m	JS	maximum

^a - DLL: D.L.Lambert, NKR: N.K.Rao, SB: S.Balachandran, DY: David Yong, BER: B.E.Reddy, JS:Jennifer Simmerer

as representative of the undisturbed stellar atmosphere and is compared with spectra obtained on other occasions. In sharp contrast, many lines in the 2000 June 16 spectrum appear double with the dominant component accompanied by a weaker component to the red (Figure 3). Affected in this way are lines of Si I, Ca I, Sc II, Fe I, and Fe II. In contrast, lines of C I, O I, and Si I, all of high excitation, do not show the red component (Figure 4). Lines which appear double are increased in equivalent width over the value when single and symmetric by no more than about 10%. Thus, it appears that the line doubling is not due to incipient emission emerging in a single stronger and broader line. Emission lines are not seen in either of the spectra at maximum light.

The spectrum obtained on 2003 June 13, also at maximum light shows line doubling, but with the weaker component shifted to the blue of the principal line by about 5 km s⁻¹ (Figure 3 - panel (b)). Low excitation lines (e.g., Ba II 6141 Å, and Ca I 6162 Å) are much stronger and even show a redward extension. High-excitation lines remain unaffected except for a suggestion of a blueshifted component to C I and O I lines. Line doubling is also seen in the 1997 June 22 spectrum obtained during a minimum. That the characteristics of the doubling on 2000 June 16 and 1997 June 22 are similar suggests that the photospheric pulsation is present during a decline. Interruption of the pulsation on or about the time of onset of a decline is a possibility testable only by very intensive spectral coverage.

The mean radial velocity has been reported as -7.9 km s⁻¹ by Lawson & Cottrell (1997) and -8.7 km s⁻¹ by Herbig (1995, private communication). However, Skuljan & Cottrell (2002) while discussing the V CrA minima of 1994–1998 mention that the mean radial velocity at light maximum is -11 ± 2 km s⁻¹. The radial velocity is variable, presumably a reflection of an atmospheric pulsation, with a range of about 13 km s⁻¹ on a timescale of about 50 to 110 days according to Lawson & Cottrell (1997). Herbig’s measurements suggest a range of about 30 km s⁻¹. Our heliocentric radial velocities of the various components for the dates of observation shown in Table 2 are consistent with the published mean value and the amplitude of the variation. The velocity from high excitation lines unaffected by line doubling in the 2000 June 16 spectrum is -12 km s⁻¹, a value close to the extreme of the previously reported range. The principal component of the doubled lines in this spectrum is at this velocity (-12.6 km s⁻¹). The weaker red component is at about +3.6 km s⁻¹ or displaced by about +11 km s⁻¹ from the systemic velocity. The spectrum of 2003 June 13

shows the principal component at a radial velocity of -4 km s⁻¹ and the blueshifted components occur at -18.8 km s⁻¹, a displacement of -11 km s⁻¹ from the mean.

Line doubling not previously reported for V CrA is not unknown for RCBs, see, for example, RY Sgr (Danziger 1963; Cottrell & Lambert 1982a; Clayton et al. 1994). How common line doubling is among RCBs is unknown given the paucity of high-resolution spectroscopic observations. Line doubling is suggested to be a sign of shock wave propagation. Since the sound speed in the atmospheres of these RCBs of T_{eff} 6500K is less than 10 km s⁻¹, amplitudes exceeding these velocities are expected to produce shocks. Based on Herbig’s (1995) radial velocity measurements of V CrA which showed a range of 30 km s⁻¹, Lawson et al (1991) anticipated that V CrA would show evidence for shock waves. Although line doubling showing inflow and outflow is present with a range in velocity of at least 22 km s⁻¹, more high resolution spectroscopic observations are needed to trace the shock through the pulsation cycle. If we assume the average photometric period of 75 days is valid, the epochs of blue and redshifted components in Table 2 are separated by about half the period.

3.3 Abundance Analysis

In the earlier comprehensive abundance analysis of RCBs (Asplund et al. 2000), the analysis for V CrA was based on a spectrum of lower resolution and signal-to-noise than those available here. Therefore, we undertook an abundance analysis using the maximum light spectrum of 2003 September 6. The maximum light spectra of 2000 June 16 and 2003 June 13 were not considered because many lines are doubled in these spectra.

The abundance analysis of V CrA followed procedures developed by Asplund et al. (2000). The analysis used the line-blanketed hydrogen-deficient model atmospheres described by Asplund et al. (1997a). An abundance ratio C/He = 1% by number of atoms was assumed. Ionization equilibrium was demanded using Fe I/Fe II, Mg I/Mg II, Ca I/Ca II and Si I/Si II to provide loci in the T_{eff} - log g plane. Excitation equilibrium through the use of [O I] and high-excitation O I lines provides a gravity-insensitive temperature indicator. We also used the recipe suggested by Asplund et al. (2000) which adopts a M_{bol} of R CrBs to obtain a relation between T_{eff} and log g . The adopted parameters are indi-

Table 2. Radial Velocities (km s⁻¹) of various features in V CrA spectrum at various times.

Feature	Date						
	1989 Jul 16	1992 May 22	1996 May 11	1997 Jun 22	2000 Jun 16	2003 Jun 13	2003 Sept 6
	min	min	min	min	max	max	max
Absorption lines:							
Stellar lines	-11.6(35) ±2.2	-11.0(24) ^c ±2.2	-10.3(33) ±1.5	-5.6(18) ±0.5	-12.6(42) ±1.7	-4.1(18) ±1.1	-7.5 (25) ±1.2
Shifted Comp.				4.0 (27) ±1.3	3.6 (22) ±0.5	-18.8(31) ±2.3	
Phillip C ₂ (3,0)				-10.2(8) ±1.8			
Sharp emissions:							
	-4.9 (5)			4.4 (2)			
Absorption Components:							
(Shell)							
Na I D	-123	-277	-213 -183	-220 ^b -190 -160 -154			
K I			-214	-220 -194			
Broad Na I emission	-85 to 103 ^a		-123 to 103				

^a The emission is affected by shell absorption on the blue side.

^b The absorption extends from -240 to -130 km s⁻¹.

^cThe number given in parentheses refers to the number of lines used

cated in Figure 5 along with the loci of various indicators in the T_{eff} and $\log g$ plane.

The stellar parameters $T_{\text{eff}}=6500\pm150$ K, $\log g=0.5\pm0.3$ (cgs units) were chosen from Figure 5. A microturbulence $\xi_{\text{tur}} = 7.0\pm1.0$ km s⁻¹ was found by the customary requirement that lines of a given species provide an abundance that is independent of equivalent width. The derived abundances are given in Table 3 along with the solar abundances from Lodders (2003). Differential abundances with respect to the Sun are given as [El] and [El/Fe]. The sensitivity of the abundances to a change of T_{eff} by 250 K and $\log g$ by 0.5 dex is also given. The abundances are in good agreement with those listed by Asplund et al. (2000) except for three elements H, N and O. The present analysis utilises more unblended lines than were used earlier and also provides an upper limit to the abundance of lithium.

Our abundance analysis fully confirms Lambert & Rao's (1994) identification of V CrA as a member of their 'minority' class for RCBs. Indeed, the identification is evident from direct inspection of the spectrum: i.e., Si I lines are numerous and strong and Fe I and Fe II lines are weak relative to their strengths in a majority RCB of comparable temperature. A mark of a minority RCB is a low Fe abundance but a near-solar abundance of Si and S: Table 3 shows that [Si/Fe] \simeq [S/Fe] \simeq 2, both remarkable ratios.

3.4 The $^{12}\text{C}/^{13}\text{C}$ ratio

The $^{12}\text{C}_2$ Swan bands are fairly strong in the spectrum of V CrA at maximum light; bandheads of the 0-0 band at 5165 Å, the 1-0 band at 4737 Å, and the 0-1 band at 6174 Å are readily identified. An absorption feature near 4745 Å (Figure 5) coincides with the $^{13}\text{C}^{12}\text{C}$ 1-0 bandhead. The 4747 Å feature is similarly strong in the spectrum of Sakurai's object (V4334 Sgr) for which a low $^{12}\text{C}/^{13}\text{C}$ ratio has been demonstrated (Asplund et al. 1997b). This feature is, however, not present in spectra of either V854 Cen or R CrB, RCB stars with C₂ bands of comparable strength to those in V CrA.

We synthesized the 4732–4746 Å interval that includes the $^{13}\text{C}^{12}\text{C}$ and the $^{12}\text{C}^{12}\text{C}$ 1-0 bands. The line list kindly supplied by Martin Asplund was used previously to estimate the $^{12}\text{C}/^{13}\text{C}$ ratio for Sakurai's object. The $^{12}\text{C}^{13}\text{C}$ lines of the 0-0 and 0-1 bands and others in these sequences are present but intermingled with $^{12}\text{C}^{12}\text{C}$ lines. The vibrational isotopic wavelength shift places the 1-0 $^{12}\text{C}^{13}\text{C}$ bandhead to the red of the blue-degraded $^{12}\text{C}^{12}\text{C}$ and so provides a fine 8 Å interval for synthesizing $^{12}\text{C}^{13}\text{C}$ lines free of blending with $^{12}\text{C}^{12}\text{C}$ lines.

Spectrum syntheses for V CrA are shown in Figure 6 for the 2003 September 6 maximum light spectrum. These use the model atmosphere and abundances listed in Table 3 and different $^{12}\text{C}/^{13}\text{C}$ ratios. The C I and molecular C₂ lines are fitted with the same C abundance. A fit was also made to the 2000 June 16 spectrum in which low excitation

Table 3. Elemental Abundances for V Cr A

Species	Log ϵ_*		$\delta T_{\text{eff}}, \delta \log g$ 250 K, 0.5	n ^a	Sun ^b	[El] ^c	[El/Fe]
	Asplund et al.	present					
H I	8.0	8.68	0.17, 0.09	1	12.00	-3.3	-1.3
Li I		<0.9		1	3.35		
C I	8.6	8.79 \pm 0.37	0.01, 0.01	13	8.46	0.3	2.3
N I	8.6	8.03 \pm 0.54	0.15, 0.10	5	7.90	0.1	2.1
O I	8.7	7.78 \pm 0.22	0.11, 0.06	5	8.76	-1.0	1.0
Na I	5.9	5.67 \pm 0.03	0.14, 0.10	2	6.37	-0.7	1.3
Mg I	6.6	6.60 \pm 0.28	0.14, 0.09	4	7.62	-1.0	1.0
Mg II		6.81	0.08, 0.06	1		-0.8	1.2
Al I	5.3	5.35 \pm 0.22	0.13, 0.12	2	6.54	-1.2	0.8
Si I	7.6	7.54 \pm 0.40	0.15, 0.10	12	7.61	-0.1	1.9
Si II		7.85 \pm 0.30	0.12, 0.10	3		0.2	2.2
S I	7.5	7.23 \pm 0.12	0.04, 0.08	7	7.26	0.0	2.0
K I		4.81	0.22, 0.16	1	5.18	-0.4	1.6
Ca I	5.1	5.22 \pm 0.30	0.20, 0.09	7	6.41	-1.2	0.8
Ca II		5.48	0.02, 0.06	1		-0.9	1.1
Sc II	2.8	2.98 \pm 0.12	0.11, 0.05	3	3.15	-0.2	1.8
Ti II	3.3	3.30 \pm 0.17	0.07, 0.10	3	5.07	-1.7	0.3
Fe I	5.5	5.50 \pm 0.38	0.20, 0.10	13	7.54	-2.0	0.0
Fe II		5.54 \pm 0.41	0.02, 0.15	8		-2.0	0.0
Ni I	5.6	4.87 \pm 0.32	0.14, 0.06	4	6.29	-1.4	0.6
Zn I	2.9	3.9		1	4.70	-0.8	1.2
Y II	0.6	1.06 \pm 0.19	0.08, 0.08	4	2.28	-1.2	0.8
Zr II		1.43 \pm 0.37	0.06, 0.10	3	2.67	-1.2	0.8
Ba II	0.7	0.30 \pm 0.28	0.22, 0.04	3	2.25	-2.0	0.0

^a n = number of lines used in the analyses

^b Recommended abundances for the solar system from Lodders (2003, Table 2).

^c [El] = log ϵ_* - log ϵ_{\odot}

atomic lines exhibit line doubling but the molecular lines appear not to be doubled. Both spectra suggest a $^{12}\text{C}/^{13}\text{C}$ ratio of 3 to 4.

By way of a check, we synthesised the 4732–4746 Å interval to fit McDonald spectra of Sakurai’s object rich in ^{13}C . Synthesis for Sakurai’s object confirms that the $^{12}\text{C}/^{13}\text{C}$ ratio is low: syntheses with ratios of 2 and 5 are shown in Figure 7.[†]

3.5 The stellar wind

Clayton et al. (2003) reported a weak P-Cygni profile for the He I 10830 Å line at maximum light in V CrA suggesting a shell of hot gas moving outward with a velocity of 295 km s⁻¹. The source of excitation for the hot gas and its connection to the photosphere of the star are not clear. Rao, Lambert & Shetrone (2006) showed that in R CrB the strong photospheric lines, particularly the O I 7771 Å line, had a pronounced blue wing suggesting mass loss with an expansion velocity of 120 km s⁻¹. The O I line provides the link between the hot gas responsible for the He I line and the stellar photosphere. V CrA and R CrB show similar profiles of the O I 7771 Å line. Figure 8 illustrate the profiles on three

occasions at maximum light and two occasions at minimum light.

The stellar wind for RCBs including V CrA will be discussed in a future paper but it is significant to note that, since the stellar wind profiles are detected on all relevant spectra of V CrA, the wind is possibly a permanent characteristic. We do not have observations of V CrA during the early decline from maximum light. Observations at the 1995–1996 minimum of R CrB suggest that the wings of the O I lines are undisturbed even though the core is affected by transient emission in the early decline (Rao et al. 1999)

Another permanent feature in the maximum light spectrum of V CrA seems to be emission cores in the Ca II triplet lines. The 8498 Å line is in the gap between orders and the 8662 Å line is affected by terrestrial OH lines. Figure 9 illustrates the profiles of the 8542 Å line during three occasions at maximum light and at minimum light in 1997 June. The profiles of the line at maximum light appear to be similar to an absorption core at stellar velocity flanked by emission peaks approximately symmetrically placed at -52 and +40 km s⁻¹ relative to the stellar velocity of -7.5 km s⁻¹. The emission strength might be variable slightly but appears to be a permanent feature and unaffected by the appearance of line doubling. The only profile obtained at minimum light shows no emission peaks but the presence of a 14.5 km s⁻¹ redshifted absorption component. The profile is reminiscent of chromospheric emission and very similar to the profiles seen in R CrB at light maximum (Rao, Lambert & Shetrone 2006). Perhaps, this emission comes from the base of the stellar wind.

[†] Spectrum synthesis was undertaken for V854 Cen. A model with C/He of 1% and the abundances listed by Asplund et al. (1998) provides a fit to both the C₂ and C I lines. Syntheses suggest a lower limit of $^{12}\text{C}/^{13}\text{C}$ of 30 for V854 Cen (Rao 2005).

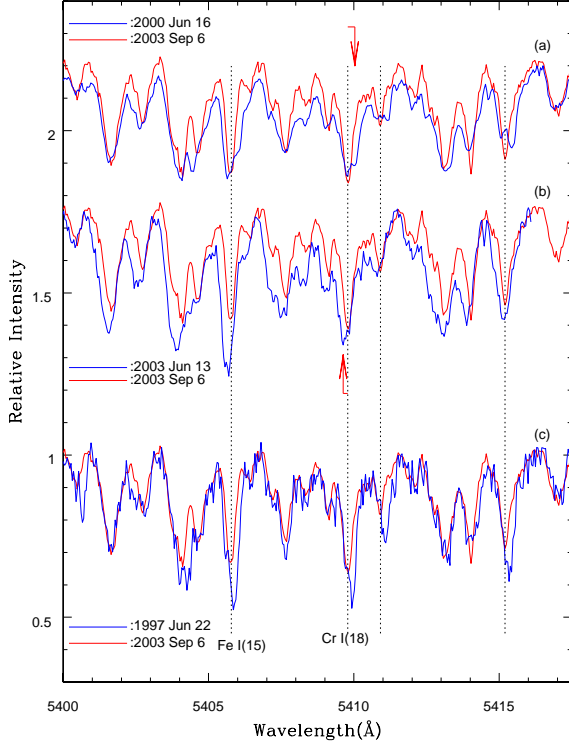


Figure 3. Absorption line spectrum of V CrA near 5410 Å. The spectrum of 2003 September 6 appearing in panels (a), (b), and (c) is taken as the normal undisturbed spectrum at maximum light. This spectrum is compared with maximum light spectra (panels (a) and (b)) and a spectrum obtained at minimum light (panel (c)) that show line doubling. Panel (a) shows that, in the spectrum obtained on 2000 June 16, many absorption lines have a weak component on the redside of the principal line. In panel (b), on the other hand, the spectrum obtained on 2003 June 13 shows the weaker absorption component on the blue side. The arrows on top and bottom of panels (a) and (b) highlight the red and blue components for the Cr I 5409 Å line. Panel (c) shows line doubling, particularly in low excitation lines, in the spectrum obtained on 1997 June 22 during a deep light minimum.

4 SPECTRUM AT MINIMUM LIGHT

For R CrB and other well observed RCBs in decline, emission lines dominate the optical spectrum. Two broad classes of emission lines are present: a rich set of sharp lines (FWHM $\sim 12 \text{ km s}^{-1}$), and a sparse and diverse set of broad lines (FWHM $\sim 300 \text{ km s}^{-1}$) (Herbig 1949; Payne-Gaposchkin 1963; Alexander et al. 1972; Rao et al. 1999). Sharp lines, primarily low-excitation transitions of singly-ionized and neutral metals, appear very early in the decline and disappear late in the recovery to maximum light (Rao et al. 1999). The broad lines, which are seen only when a RCB has faded by several magnitudes, may include lines of the He I triplet series, Ca II H and K, K I resonance lines at 7664 Å and 7699 Å, Na I D lines, [O II], and [N II] lines, i.e., a mix of high and low excitation lines with similar but differing profiles (Rao et al. 1999). The range of excitation/ionization of these carriers and the differing velocity and width of the profiles suggests that there may be perhaps three regions and/or excitation mechanisms responsible for the broad emission lines.

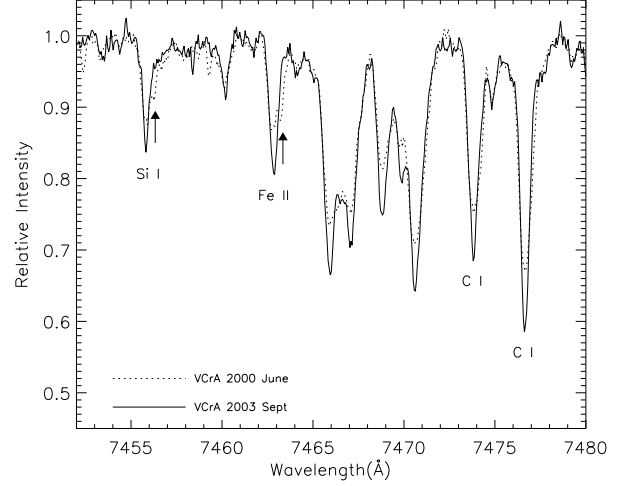


Figure 4. Spectrum of V CrA near 7465 Å at maximum light on 2003 September 9 (full line) and 2000 June 16 (dotted line). Note the presence in the latter spectrum of redshifted absorption components to the lines of Si I and Fe II and their absence for lines of C I.

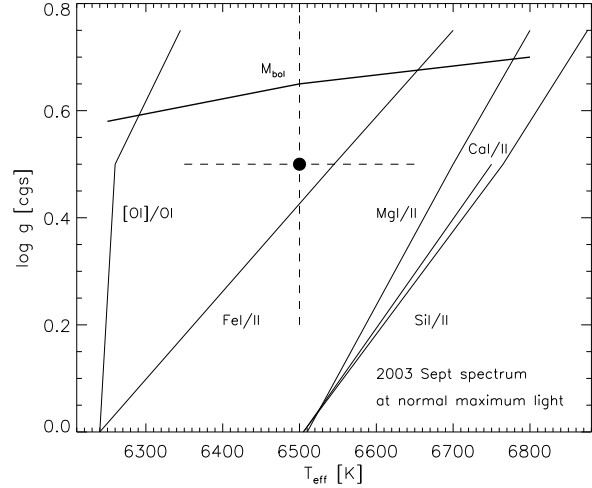


Figure 5. Loci of ionization equilibria and other parameters in T_{eff} and $\log g$ plane from the spectrum on 2003 September 6. The final choices of T_{eff} and $\log g$ are indicated by the large dot.

The photospheric absorption line spectrum may also change during a decline. In deep minima, the photospheric absorption lines may be ‘veiled’, i.e., the lines become very shallow and broad. New absorption features may also appear. Broad blueshifted absorption (‘shell’) components have been seen to accompany commonly the Na D lines, and occasionally the K I 7664 Å and 7699 Å resonance lines, and the Ca II H and K lines. The Na D absorption components appear especially at and following minimum light. The ubiquity of the sharp and broad emission and the blue-shifted absorption Na D lines across the sample of RCBs is unknown at present. Probably, the sharp emission lines of ionized and neutral metals are a common feature of all declines of all

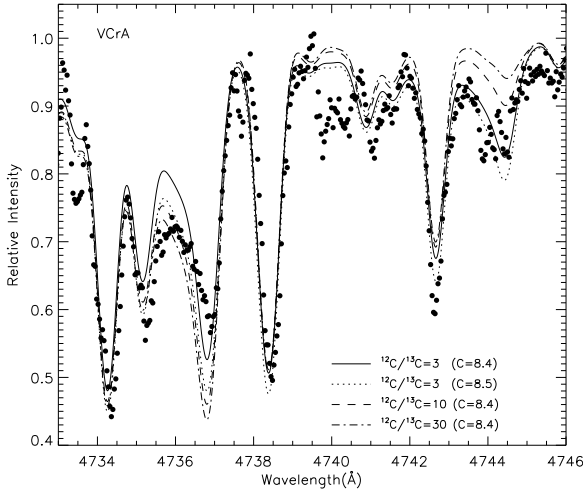


Figure 6. The spectrum of V CrA in the region of the $^{12}\text{C}^{12}\text{C}$ (4736.5 Å) and $^{12}\text{C}^{13}\text{C}$ (4744.7 Å) 1-0 Swan bandheads. The observed spectrum on 2003 September 6 is shown as dots. The lines show the synthetic spectrum for various ratios of the $^{12}\text{C}/^{13}\text{C}$ ratio.

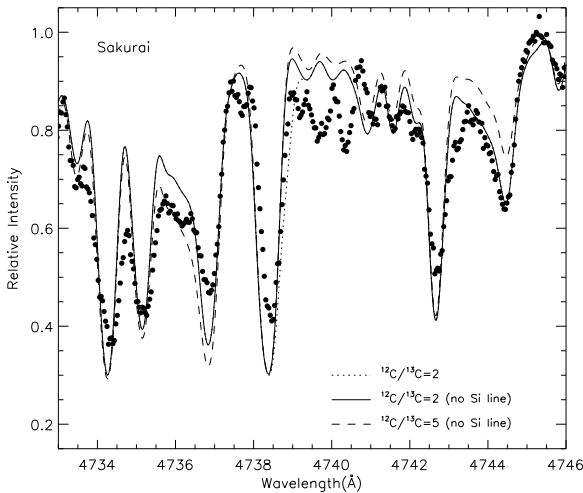


Figure 7. The spectrum of Sakurai's object on 1997 October 7 (dots) in the region of the $^{12}\text{C}^{12}\text{C}$ and $^{12}\text{C}^{13}\text{C}$ 1-0 Swan bandheads and synthetic spectra for various $^{12}\text{C}/^{13}\text{C}$ ratios (Asplund et al. 1997b).

RCBs (Skuljan & Cottrell 2004).[‡] Since few RCBs have been observed in deep minima, reported sightings of broad lines are rare. One observation worthy of particular note, if applicable to all RCBs, is Whitney et al.'s (1992) discovery that the Na D broad emission from V854 Cen is unpolarized at a time when the continuum is markedly polarized. This suggests that during a decline the stellar continuum is seen only in the reflected light where as the Na D broad emission region is viewed directly.

[‡] Emission lines of C I and O I first seen early in R CrB's 1995 decline may have been missed in other declines of R CrB and other RCBs simply for lack of appropriate observations at early times.

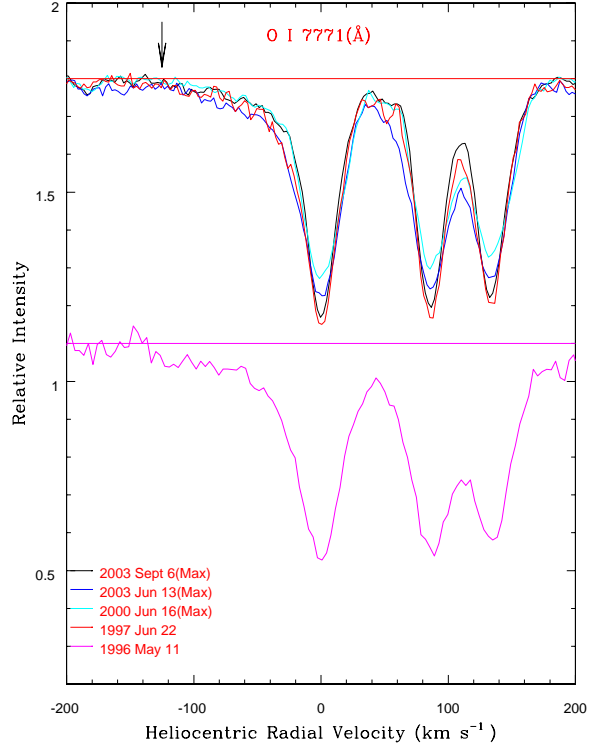


Figure 8. Profiles of the O I triplet lines at 7774 Å. Zero radial velocity here corresponds to the stellar velocity of the 7771 Å line. The top panel illustrates the profiles obtained from McDonald spectra on three occasions at maximum light and at minimum on 1997 June 22. The bottom panel illustrates the same lines obtained at a lower resolution at CTIO during the light minimum in 1996 May. Note the pronounced blue wing extending to the a radial velocity of -125 km s⁻¹ relative to the star (shown by the arrow) on all occasions.

4.1 Spectra of V CrA at minimum light

Our collection of high resolution spectra sample four light minima over 8 years. We obtained one spectrum in each minimum mostly at the beginning of light recovery phase. We present a description of these spectra.

1989 July 16 : The spectrum was obtained after about 288 days since the beginning of the minimum. The star reached a minimum magnitude of 13.8 and was observed near minimum. The spectrum is mostly in absorption with few sharp emissions seen in the centres of deep absorption lines. Lines of Sc II, and Ba II are in emission. Only one Sc II 6604 Å line is seen above the continuum in the spectral region covered (Figure 10). The sharp emission lines are all of low excitation. An unusual aspect of the sharp emissions in this spectrum is that they are redshifted relative to the absorption lines (Table 2); a blueshift of a few km s⁻¹ is common among other RCBs.

The absorption lines are less strong than at maximum light. Unlike R CrB where the Na I sharp emission line is very strong, the sharp emission at Na D is inconspicuous for V CrA. The weak broad Na I D emission extends symmetrically relative to the stellar velocity (Figure 11) extending to

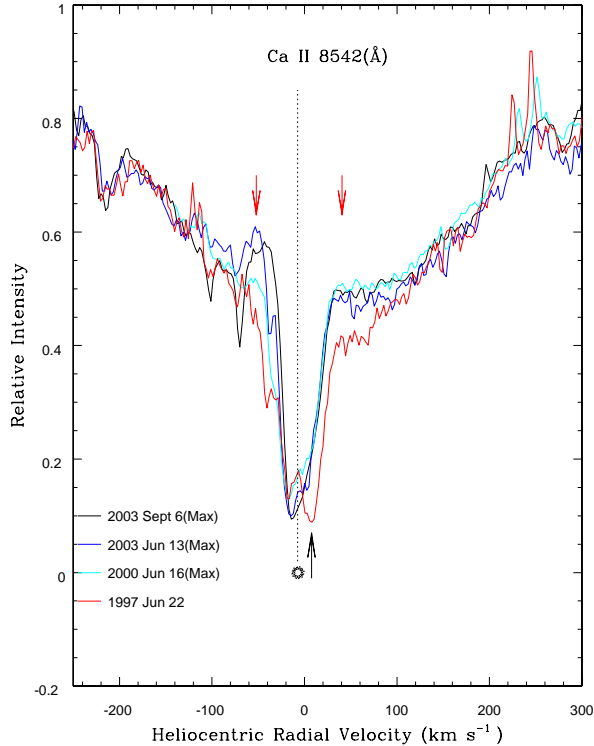


Figure 9. The profiles of Ca II 8542 Å line on three occasions at maximum light and during the minimum in 1997 June (red line). All three maximum profiles look similar. The centre of the line shows an asymmetrical absorption core flanked by emission bumps on either side (marked by red arrows pointing down). The profiles are aligned to the stellar absorption lines of the 2003 September 6 spectrum; the vertical dashed line refers to the stellar velocity. The minimum profile does not show the emission bumps instead it shows an extra absorption component (marked by an arrow pointing upwards) redward of the stellar radial velocity (the blue side of the profiles has terrestrial water vapour lines superposed).

about $\pm 100 \text{ km s}^{-1}$. There is an indication of shell absorption present at -120 km s^{-1} for the Na I D lines.

1992 May 22: When this spectrum was obtained, V CrA was less than a magnitude below maximum light and the ensuing minimum was shallow attaining a maximum depth of just 1.8 magnitudes. Not surprisingly perhaps, the spectrum is very similar to that at maximum light. A comparison (Figure 10) of the 2003 September 6 maximum light spectrum (after smoothing for the resolution difference) with the 1992 May 22 spectrum shows a very good match except for very low-excitation absorption lines and C₂ Swan bands which are stronger. Weak shell absorption in the Na I D lines seems to be present at -270 km s^{-1} , a remnant of ejected gas from earlier minima.

1996 May 11: V CrA was well into a prolonged minimum that started about 280 days before our observation and covered three declines and partial recoveries without reaching its usual maximum brightness (Figure 1). The spectrum was obtained at the beginning of the first recovery phase. It mostly shows an absorption spectrum similar to that of maximum light spectrum except for the presence of broad

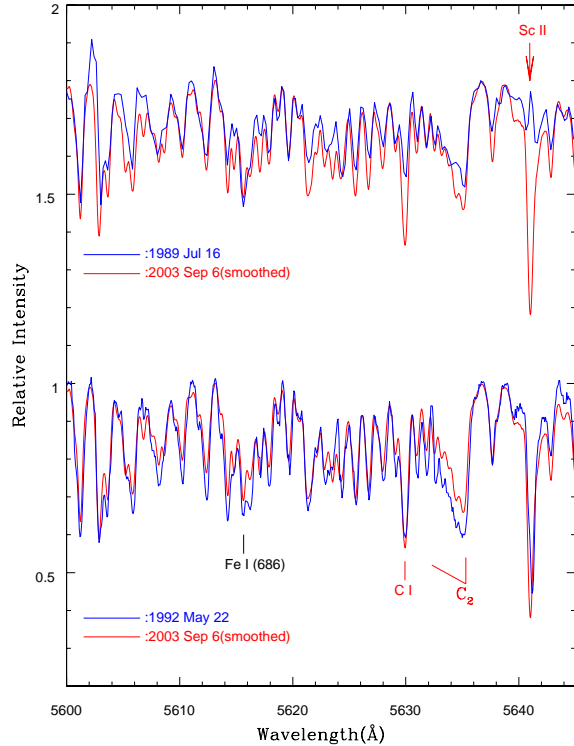


Figure 10. The minimum light spectra of 1989 July 16 and 1996 May 22 are compared with the maximum light spectrum obtained on 2003 September 6 (red line) after smoothing to the same resolution. The sharp emission in Sc II line in the 1989 spectrum is shown by the arrow. Most of the absorption lines are of lower depth in the 1989 spectrum relative to the maximum spectrum. The 1992 spectrum obtained at a shallow minimum shows the C₂ band and low excitation lines to be enhanced in absorption but the sharp Sc II emission is effectively absent.

Na I D emission lines and strong shell absorption at -215 km s^{-1} for lines of Na I D (Figure 11) and K I. A comparison with R CrB during its 1995–1996 minimum is shown in Figure 12 for the Na I D₂ and the K I 7698 Å lines. The spectra of R CrB and V CrA were obtained about 220 and 280 days, respectively, after the initial drop in light. Obviously, the very strong sharp Na I D emission in R CrB is missing in the spectrum of V CrA even though the broad emission is of similar strength. Another interesting contrast is seen for the K I line 7698 Å. The line is a normal absorption line at maximum in R CrB and the blueshifted shell absorption components, corresponding to the strong Na I D components, are not present. The line in V CrA shows blueshifted shell absorption corresponding to the Na I D lines. A striking aspect of this and other spectra of V CrA in decline is that the numerous sharp emission lines characteristic of R CrB (and other RCBs) are largely absent from V CrA (Clayton et al 1992).

1997 June 22: The spectrum was obtained on the recovery phase of the second major drop in light in the prolonged minimum that started around 1995 July. Subsequently, the star became fainter than $V \simeq 15.5$ before recovering. In most respects, the 1997 June 22 spectrum resembles a spectrum taken at maximum light. Three features

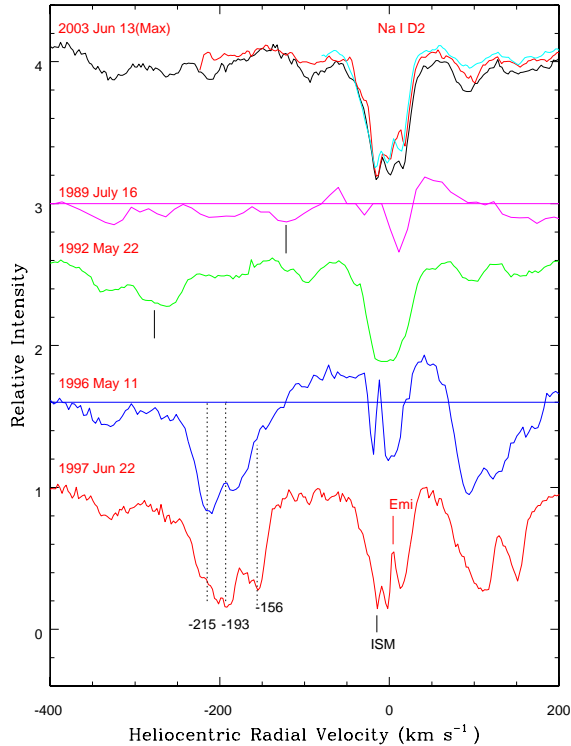


Figure 11. The profiles of Na I D2. The top spectrum shows the profiles on three occasions during maximum light (2000 June 16 (blue), 2003 June 13 (red), 2003 September 6 (black)). Slight variations in the stellar line are seen but, as expected, the interstellar (ISM) component -14.7 km s^{-1} is not variable. The other four spectra show the profile during various minima. Sharp emission in the core of the Na D line in the 1997 June 22 spectrum is identified. The position of the continuum is shown for the 1989 July 16 (magenta line) and 1996 May 11 (red line) spectra to highlight the broad emission.

not attributable to a stellar photosphere are present: (i) absorption lines of the C_2 Phillips system; (ii) the expected high velocity blue-shifted broad absorption components of the Na I D and the K I resonance lines; (iii) sharp emissions.

4.2 Absorption lines of C_2 Phillips system

Weak absorption lines of the C_2 Phillips system are present in the spectrum of 1997 June 22 (Figure 13). This system arises from the molecule's electronic ground state whereas the Swan system's lower electronic state is a low-lying electronic state (Ballik & Ramsay 1963). In dilute gas, as found in a circumstellar shell, the Phillips system is the transition of choice for detecting C_2 molecules. We measured lines of the 3-0 band in the 7760 \AA to 7880 \AA interval. This is the only spectrum in our collection to cover the 3-0 band to show these absorption lines.

A rotational temperature of $1230 \pm 30 \text{ K}$ is obtained (Figure 14) using the molecular data given by Bakker et al. (1998). The molecular column density is $2 \times 10^{15} \text{ cm}^{-2}$. The radial velocity of the C_2 molecules is -10.2 km s^{-1} suggesting an expansion velocity of 4.6 km s^{-1} relative to the velocity of the main component (-5.6 km s^{-1}) but only

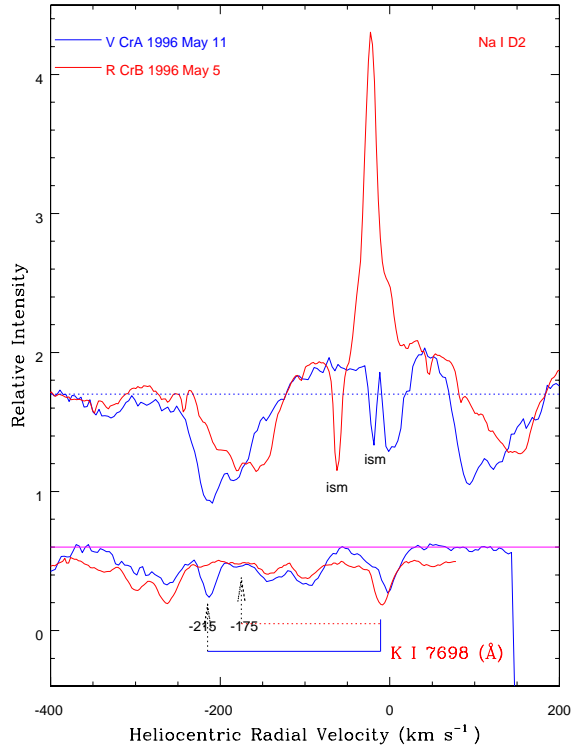


Figure 12. Comparison of the profiles of the Na I D2 and K I 7698 Å lines in V CrA (blue) and R CrB (red) obtained when both stars were 4.8 magnitudes fainter than at maximum light and recovering from a deep minimum. Note the strong blueshifted shell absorption components to the Na I D2 profiles with similar expansion velocities in both stars. The very strong sharp emission in the Na I D2 line seen in R CrB is absent in V CrA.

about 2 km s^{-1} relative to the star's systemic velocity. Presence of cool C_2 molecules suggests that the gas is at temperatures where dust may condense. Similar detections of cool C_2 molecules have been reported by us for V854 Cen (Rao & Lambert 2000) and R CrB (Rao, Lambert & Shetrone 2006).

4.3 Shell Absorption Components

Blueshifted absorption components to the Na I D lines and K I lines are common across the minimum light spectra, as noted above. The spectra of 1996 May 11 and 1997 June 22 are of particular interest as they were obtained in successive minima during a prolonged minimum. In Figures 10 and 11, the stellar Na D2 lines appear near the systemic velocity of about -8 km s^{-1} . The stellar line consists of two components on some spectra and is blended with an ISM line of constant velocity and strength. The blue-shifted shell components are several in number with velocities between about -160 km s^{-1} to -230 km s^{-1} with the strongest absorption at -190 km s^{-1} . The component at -156 km s^{-1} was not present in 1996 May 11 but emerged as an additional component in 1997 June. The K I 7698 Å line clearly shows (Figure 15) the -215 km s^{-1} component, which was strong in 1996 May and weakening by 1997 June 22 and the

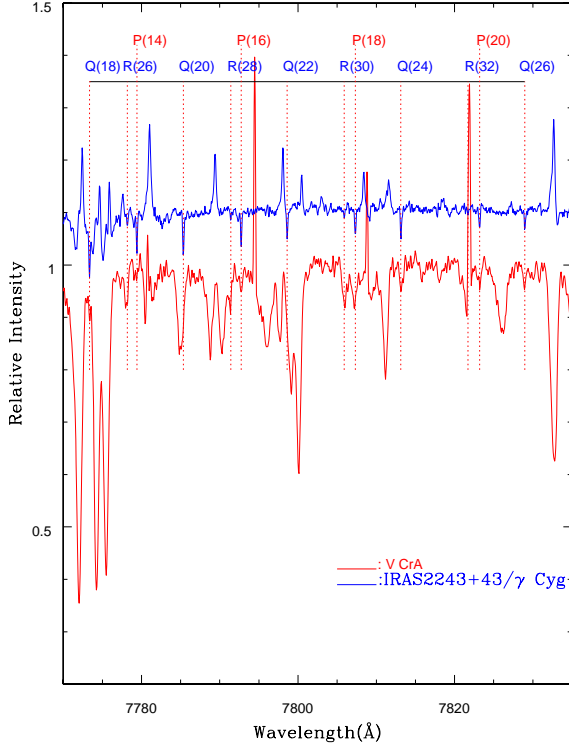


Figure 13. The spectrum of V CrA obtained on 1997 June 22 (red) is shown along with a spectrum of the post-AGB star IRAS2243+43 (blue) show the absorption lines of Phillips 3-0 system identified by the red dotted lines. The emission-like features in the IRAS spectrum are artefacts resulting from the procedure used to ratio out the telluric lines. The sharp emission lines in the spectrum of V CrA are uncompensated terrestrial OH lines.

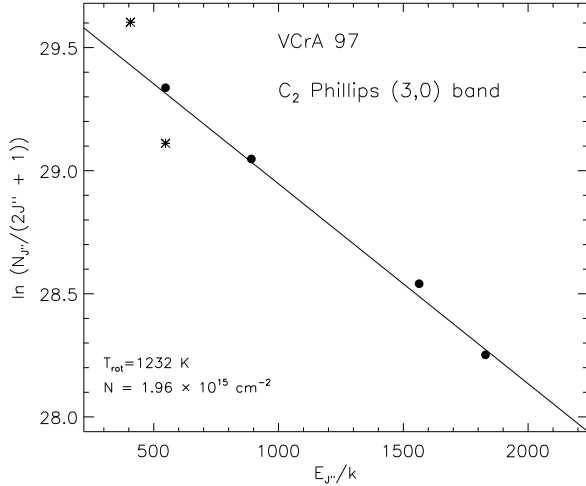


Figure 14. Boltzmann plot of the absorption lines of the 3-0 band of the C₂ Phillips system from the spectrum of V CrA obtained on 1997 June 22. Star and dot symbols refer to P and Q branch lines respectively.

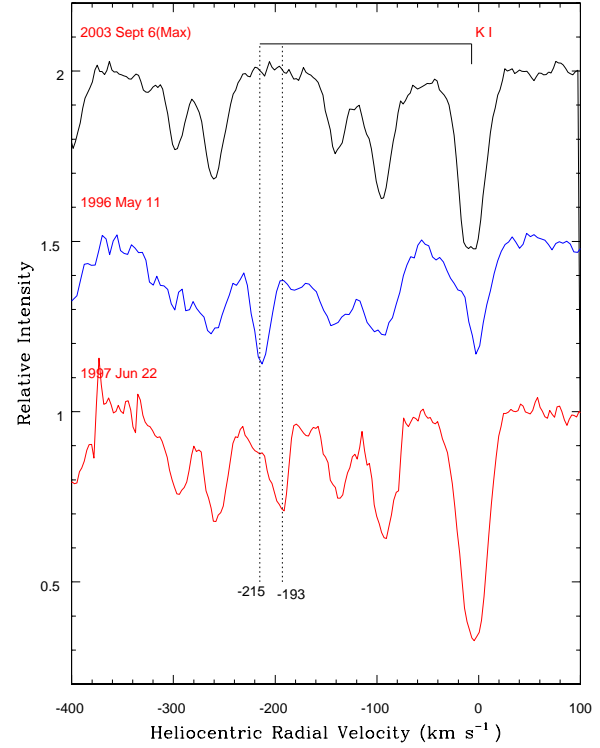


Figure 15. The profiles of K I 7698 Å line and its blueshifted shell absorption components at the 1996 and 1997 minima along with the maximum light spectrum. The shell components are absent at light maximum. Note that the component at -215 km s^{-1} which is strong at the 1996 minimum had weakened considerably by 1997 but a new shell absorption component at -193 km s^{-1} emerged in 1997. The 1996 spectrum shows the stellar K I 7698 Å line has been filled in by emission.

-193 km s^{-1} component that was not present in 1996 May appearing with greater strength in 1997 June.

Rough estimates of the column densities of Na I and K I in the velocity range -230 to -190 km s^{-1} are made by using the doublet method (Spitzer 1968). These give the abundance ratio $\log(\text{Na I}/\text{K I}) \simeq -0.4$ and -0.6 for the two parts of the profile. The photospheric abundance analysis (Table 3) gave the elemental abundance ratio as -0.4 which is fortuitously close to the ratio from the shell lines. The total column density of Na I is $9.3 \times 10^{12} \text{ cm}^{-2}$. By assuming the Na to He ratio as estimated earlier and the size of the cloud based on its velocity of expansion and its dispersion (from Na I D lines), the cloud mass is estimated as $6.9 \times 10^{24} \text{ gm}$ or $3.4 \times 10^{-9} M_{\odot}$.

4.4 Sharp Emission lines

Even during this minimum sharp emission lines, that are a characteristic of RCB stars at minimum, are only represented in the cores of Na I D lines (Figure 16) in the spectral regions observed. The possibility exists that the sharp emission region was obscured by dust and only very strong emissions (eg. Na I D) could be seen. In addition the level of excitation appears to be low in the sharp emission region such

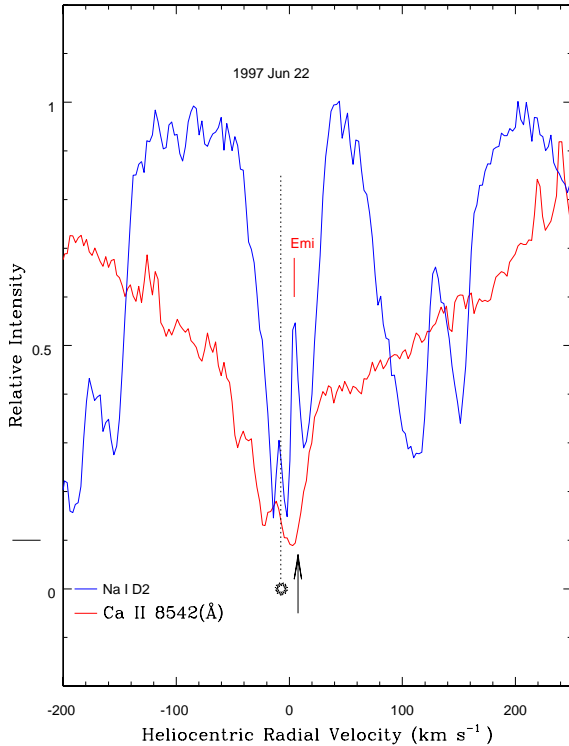


Figure 16. The profiles of the Na I D2 and Ca II 8542 Å lines from the spectrum obtained on 1997 June 22. The radial velocity scale is heliocentric. Note the sharp emission present in Na I D2 is absent from the Ca II line.

that only emission is present in Na I D lines but not in Ca II triplet lines (Figure 15). The absorption lines, particularly of low excitation, seems to have redward components (Figure 3c).

5 DISCUSSION

Important questions posed by RCB stars remain unanswered. The two most fundamental concern the origin of these H-deficient stars, and the mechanisms by which a cloud of soot forms and obscures the star. One supposes that the origins of the stars will be betrayed by examination of the abundances of the stellar atmospheres and that thorough spectroscopic and photometric scrutiny of stars from maximum light into and through declines will provide the clues to the understanding of cloud formation.

Two scenarios remain in play to account for a H-deficient luminous star. In the first, a final He-shell flash in a post-AGB star on the white dwarf cooling track creates a H-deficient luminous star that evolves rapidly to lower temperatures. This is dubbed the ‘final flash’ (FF) scenario. In the second, the H-deficient luminous star is formed from the merger of a He and a C-O white dwarf. In the close binary system with loss of energy by gravitational radiation, accretion of the He white dwarf by the C-O white dwarf leads, subject to restrictions such as the total mass should not exceed the Chandrasekhar limit, to a H-poor supergiant

with the C-O white dwarf as its core. This is dubbed the ‘double-degenerate’ (DD) scenario.

Evidence suggests that the DD rather than the FF scenario provides the superior accounting for the elemental abundances of C, N, and O for RCB stars and their likely relatives the extreme Helium (EHe) stars (Saio & Jeffery 2002; Asplund et al. 2000; Pandey et al. 2006). Convincing support for the DD scenario as creators of the cool hydrogen deficient (HdC) stars, another example of likely relatives of RCBs, is provided by Clayton et al.’s (2005, 2007) discovery that ^{18}O is very abundant in those HdC’s with strong CO vibration-rotation bands; ^{18}O may be readily synthesized by α -capture from abundant ^{14}N during the merger in the DD scenario but not made with ease in the FF scenario. Several cool RCBs also show large amounts of ^{18}O (Clayton et al. 2007) but warm RCBs such as V CrA and R CrB do not show CO bands in their infrared spectra (Tenenbaum et al. 2005). The FF scenario does plausibly account for other stars. Most notable among the FF candidates are FG Sge and V4334 Sgr, also known as Sakurai’s object and V605 Aql (Clayton et al. 2006). It is not impossible that RCBs from the FF scenario lurk among the analysed sample attributed in the main to the DD scenario.

5.1 Composition of V CrA

Our determination of V CrA’s chemical composition fully confirms the star’s status as a minority RCB with the added important information that V CrA is rich in ^{13}C . Indeed, the estimated $^{12}\text{C}/^{13}\text{C}$ ratio is equal within the measurement uncertainties to the ratio expected from running of the H-burning CN-cycle. This cycle cannot have proceeded to equilibrium because the C/N ($\simeq 5$) ratio is much greater than one instead of much less than one, as required of equilibrium abundances of C and N. One supposes that C-rich gas was mildly exposed to warm protons.

Pronounced signatures of a minority RCB are the high Si/Fe and S/Fe ratios (Lambert & Rao 1994). That these ratios are extraordinary for V CrA is shown in Figure 17 where [Si/Fe] vs [S/Fe] is plotted for V CrA (see Table 3), R CrB and V2552 Oph (Rao & Lambert 2003), other warm RCBs (Asplund et al. 2000), V854 Cen (Asplund et al. 1998), the hot RCB DY Cen (Jeffery & Heber 1993), Sakurai’s object (Asplund et al. 1997b), FG Sge (Gonzalez et al. 1998), and the extreme helium stars (EHEs) (Pandey et al. 2001, 2006; Pandey & Reddy 2006). Three of the known minority RCBs – V CrA, V3795 Sgr, and DY Cen – stand out in Figure 17 far apart from the region occupied by the RCBs and the EHEs. It is noteworthy that this trio span a wide range in effective temperature: V CrA at 6500 K, V3795 Sgr at 8000 K, and DY Cen at 19500 K. Therefore, it seems unlikely that the odd abundances are artefacts resulting from a misrepresentation of their atmospheres and systematic errors in the abundance analyses. The fourth known minority RCB is VZ Sgr which appears to form a bridge between the first three and the other RCB and EHe stars that constitute the majority of these H-poor stars. The mean [Si/Fe] = +0.5 and [S/Fe] = +0.6 of the majority RCBs are elevated by about +0.2 to +0.3 dex with respect to the values found for unevolved disk stars of the sample’s mean metallicity. The magnitude of the elevation is possibly within the range of

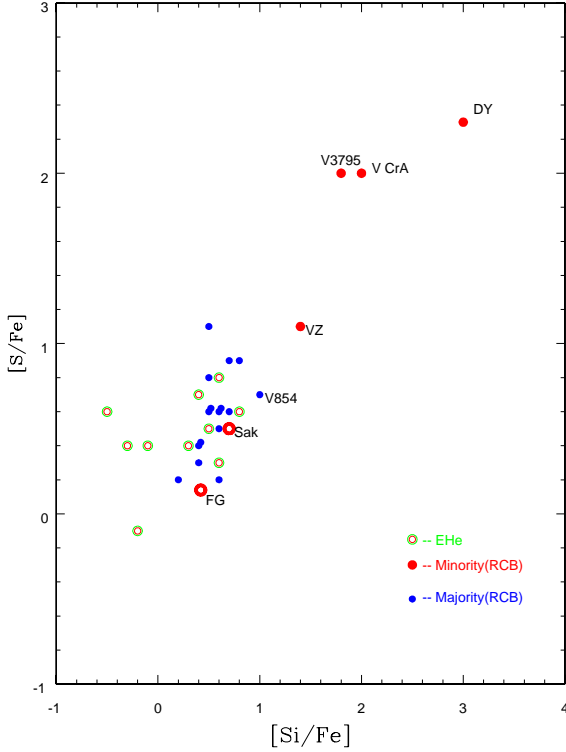


Figure 17. The abundance ratio $[S/Fe]$ vs $[Si/Fe]$ for minority RCBs (red dots, stars identified by name), majority RCBs (blue dots), EHe stars (yellow dots), and the FF candidates FG Sge and Sakurai’s object (unfilled red dots).

systematic errors incurred by use of classical model atmospheres and the assumption of LTE.

Two general comparisons of the composition of V CrA are offered in Figure 18. In the top panel, the abundance differences are presented between V CrA and the mean of the majority RCBs from Asplund et al. (2000). This comparison may reduce the effect of the carbon problem uncovered and discussed by Asplund et al. (2000). The relative overabundance of Si, S, Sc and possibly Ca is seen. These elements aside there is a general and roughly uniform underabundance of elements in V CrA with respect to the mean abundances of the majority RCBs. In the lower panel, the comparison is between V CrA and the solar system (Lodders 2003). Here, Si, S, and Sc stand out as overabundant in V CrA. As seen from Figure 18, the ratio of Si/Fe and S/Fe far exceed the normal enhancement expected of a metal-poor star. This exceptional excess does not apply to Mg, Ca, and Ti which in normal metal-poor stars share the small excess seen by Si and S (say, $[El/Fe] \simeq +0.3$). (C, N, and O in V CrA and all RCBs were altered in the course of stellar evolution.) The other minority RCBs – V3795 Sgr, VZ Sgr, and DY Cen – resemble V CrA in composition. V3795 Sgr is a close twin of V CrA but for a lower H abundance by at least four orders of magnitude.[§] VZ Sgr is very similar to V

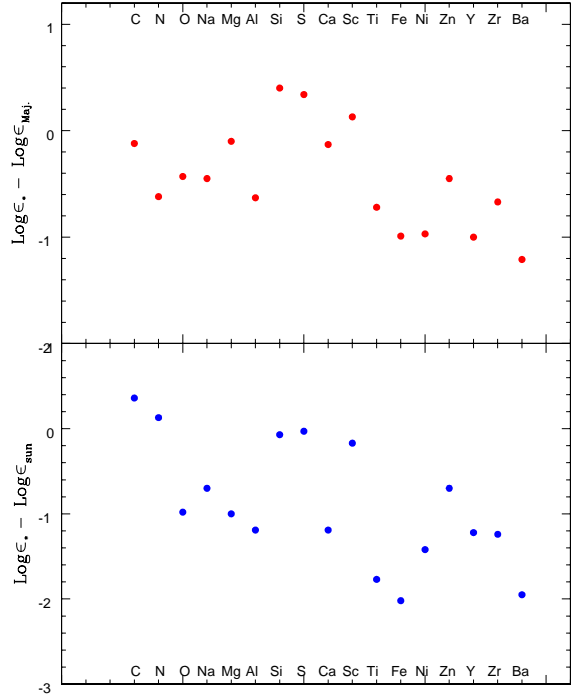


Figure 18. The composition of V CrA. In the top panel, abundance differences (in dex) are given for V CrA relative to the mean of the majority RCBs from Asplund et al. (2000). In the bottom panel, abundance differences (in dex) are given for V CrA relative to the solar system abundances from Lodders (2003).

CrA but for lower $[Si/Fe]$ and $[S/Fe]$ and a clear enrichment of the *s*-process elements Y, Zr, and Ba.

An intriguing clue to the origin of minority RCBs may be the demonstration here that V CrA is rich in ^{13}C . In contrast, the warm majority RCBs probably, the cool RCBs certainly, and the HdC stars also certainly are not ^{13}C -rich; see, for example, Cottrell & Lambert (1982b), Warner (1967), Clayton (1996), Tenenbaum et al. (2005), and Clayton et al. (2007). Most unfortunately, the minority RCBs V3795 Sgr and DY Cen are too hot to provide detectable C_2 bands and, hence, it is unknown whether their atmospheres are as rich in ^{13}C as is V CrA’s. It might be supposed that synthesis of ^{13}C in the case of V CrA may be related to survival of hydrogen in its atmosphere, the H abundance, although depressed by four orders of magnitude from its assured initial value, is about two orders of magnitude greater than in other warm RCB stars. Yet, V854 Cen with a factor of ten more hydrogen is not ^{13}C -rich: $^{12}C/^{13}C \geq 30$ is the limit we set from the 1-0 Swan band.

With the separation of the minority stars from the majority, it is difficult not to suspect that the minority followed an evolutionary path with a branch or major diversion not open to the majority. The similarity in abundances among the minority stars suggests that, whatever the path, it led

[§] The Ni abundance in Table 3 is 0.7 dex lower than that given

by Asplund et al. With this abundance, V3795 Sgr has a Ni abundance that is 0.9 dex higher than that of V CrA.

to definitive abundances for Si, S, and Sc for the traveller. Events along the minority's path may have been a mixture of nuclear and chemical effects. The low $^{12}\text{C}/^{13}\text{C}$ ratio is an example of a nuclear effect perhaps specific to the minority stars; majority RCBs showing strong Swan bands do not show a detectable 4747 Å $^{12}\text{C}^{13}\text{C}$ bandhead. In contrast to the nuclear process betrayed by the high ^{13}C abundance, the run of abundance anomalies is not so obviously attributable to nucleosynthesis. The high (solar) abundances of Si, S, and Sc must be reconciled with lower abundances of Na, Mg, Al, Ca, Ni, Zn, Y and Zr, and even lower abundances of Ti, Fe, and Ba. This abundance pattern is shared with the other minority stars. One speculation is that the minority RCBs result from a variant of the DD scenario - for example, a He white dwarf merger with a ONeMg white dwarf, the latter resulting from an intermediate mass AGB star. Nucleosynthesis in the merger may be capable of producing Si and S from the mixing of He with the surface of the ONeMg white dwarf. An intriguing observation of possible relevance is that analyses of the ejecta of ONeMg novae have shown several examples with Si enhancements and one with a S enhancement; sulphur lines are generally not detected. For V838 Her, Schwarz et al. (2007) reported Si and S enriched by factors of 5 and 22, respectively, with no enhancement of Mg. Elements heavier than S were not reported but Al was found to be overabundant by a factor of 18, an enrichment counter to the results for the minority RCBs.

The pattern is not obviously attributable to a chemical effect such as is the case with the dust-gas separation process that creates abundance anomalies seen in some RV Tauri variables (Giridhar et al. 2005). Affected RV Tauri with an oxygen-rich atmosphere provide an abundance pattern that is not that shown by the minority RCBs. The minority stars presently have a carbon-rich atmosphere. The difference between O-rich and C-rich gas results in grains of different composition (e.g., silicate vs graphite) forming from cool gas and, hence, different compositions for the remaining gas. If the dust-gas separation were to operate in gas from the RCB star, such that SiC grains should be abundant and their expulsion from gas would result in a Si *underabundance* when gas was accreted by the star. The ISO spectra of the three RCB stars observed R CrB, RY Sgr and V854 Cen do not indicate any features attributable to SiC grains (Lambert et al 2001). The puzzle of the minority RCBs' abundance anomalies remains.

5.2 The sooty outer atmosphere

A stellar wind, as sensed by the He I 10830 Å and O I 7771 Å profiles, is fed by the atmosphere. In addition, pulsations are present during light maximum with mild shocks propagating through the atmosphere as evidenced by the line doubling. The shocks may feed the stellar wind. Probably, when a strong shock occurs the post-shocked region might reach temperature sufficiently cool for the dust to condense (Woitke et al. 1996). How the dust grains grow and clouds form is not quite clear; Woitke (2006) and Woitke & Niccolini (2004) have modelled dust formation in carbon-rich AGB stars. Radiation pressure on dust grains and dust-gas collisional coupling lead to ejection of clouds that are seen by the shell blue-shifted absorption components of the Na I D and other lines. These components seen in spectra taken at

minimum and during recovery to maximum are a common feature of majority RCBs and apparently too of minority RCBs (Rao et al. 1999). The absorbing gas would appear to be associated with the dust causing the ongoing decline.

Presence of C_2 molecules at low rotational temperatures may also be a common and not unexpected feature of RCBs in decline. In addition to their detection here in V CrA, the molecules have been detected for V854 Cen (Rao & Lambert 2000) and R CrB (Rao, Lambert, & Shetrone 2006). In all cases, the velocity of the C_2 molecules is low relative to the systemic velocity. Molecules have not been detected accompanying the high-velocity Na atoms.

Spectra described here show differences in the emission line spectrum at minimum light between V CrA and well studied majority RCB stars, particularly R CrB and RY Sgr. Especially noticeable is the weakness of the sharp emission lines (relative to the stellar continuum) from V CrA, as highlighted by the absence of a sharp emission component to the Na D lines. Since the location of the emitting region is uncertain for even the well studied RCBs, it is difficult to interpret this seemingly unusual aspect of V CrA. The broad lines of which the Na D lines are the sole example seen in V CrA appear to be of similar strength (relative to the stellar continuum) in V CrA and R CrB (Figure 11).

The stellar absorption line spectrum seen when the star has faded by three to five magnitudes is a replica of the spectrum at maximum light; there is no indication that the spectrum is 'veiled', i.e., the absorption lines are much shallower and broader and even slightly Doppler shifted. Since such veiling was seen in the 1995–1996 minimum of R CrB only when the star was 7 or more magnitudes below maximum light, the absence of veiling for V CrA observed no more than five magnitudes from maximum may be not be a surprise. Although some clouds may be optically thick, the star may have been seen through optically thin clouds or gaps between clouds.

6 CONCLUDING REMARKS

Differences between the spectra of RCBs at minimum light encourage us to continue our monitoring of V CrA and other RCBs. Studies of the initial stages of a decline should reveal clues to the trigger that sets off a decline. In this era when photometric observations by amateur astronomers are reported on the internet almost instantaneously, spectroscopic and other follow-up observations are limited by access to suitable telescopes. The advent of queue scheduling is smoothing the path to obtaining the follow-up observations. Development of a consortium of observers would also ease the situation. Observations of the RCBs in the deepest of minima are likely to provide novel data on their extended atmospheres, especially on the enigmatic broad lines which, the Na D lines apart, have been studied in detail with high-quality spectra only in the case of R CrB. For RCBs, aside from the three brightest stars R CrB, RY Sgr, and V854 Cen, a large telescope will be needed to acquire quality spectra at the faint magnitudes expected to reveal the broad lines.

7 ACKNOWLEDGEMENTS

We acknowledge with thanks the variable star observations from the AAVSO database. This research has made use of the SIMBAD database, operated at CDS, Strasbourg, France. Our sincere thanks to Suchitra Balachandran, Jennifer Simmerer, David Yong, Eswar Reddy for securing observations at our request. We would also like to thank Martin Asplund for supplying line lists, programmes, and instructions on how to compute the C₂ bands. Thanks are due to David Yong for his assistance. This research has been supported in part by a grant from the Robert A. Welch Foundation of Houston, Texas. We would like to thank the referee, Geoff Clayton, for useful comments.

REFERENCES

- Alexander, J.B., Andrews, P.J., Catchpole, R.M., Feast, M.W., Evans, L.T., Menzies, J.W., Wisse, P.N., Wisse, M. 1972, MNRAS, 158, 305
- Asplund, M., Gustafsson, B., Kiselman, D., Eriksson, K., 1997a, A&A, 318, 521
- Asplund, M., Gustafsson, B., Lambert, D. L., Rao, N. K., 1997b, A&A, 321, 17
- Asplund, M., Gustafsson, B., Lambert, D. L., Rao, N. K., 2000, A&A, 353, 287
- Asplund, M., Gustafsson, B., Rao, N. K., Lambert, D.L., 1998, A&A, 332, 651
- Ballik, E.A., Ramsay, D.A. 1963, ApJ, 137, 84
- Bakker, E.J., van Dishoeck, E.F., Waters, L.B.F., Schoenmaker, T., 1997, A&A, 323, 469
- Clayton, G.C. 1996, PASP, 108, 225
- Clayton, G.C., Whitney, B.A., Stanford, S.A., Drilling, J.S. 1992, ApJ, 397, 652
- Clayton, G.C., Geballe, T.R., Bianchi, L. 2003, ApJ, 595, 412
- Clayton, G.C., Kerber, F., Pirzkal, N., De Marco, O., Crowther, P.A., Fedrow, J.M. 2006, ApJ, 646, L69
- Clayton, G.C., Geballe, T.R., Herwig, F., Fryer, C., Asplund, M. 2007, ApJ, 662, 1220
- Clayton, G.C., Herwig, F., Geballe, T.R., Asplund, M., Tenenbaum, E.D., Engelbracht, C.W., Gordon, K.D., 2005, ApJ, 623, L141
- Clayton, G.C., Lawson, W.A., Cottrell, P.L., Whitney, B.A., Stanford, S.A., de Ruyter, F., 1994, ApJ, 432, 785
- Cottrell, P.L., Lambert, D.L., 1982, Observatory, 102, 149
- Cottrell, P.L., Lambert, D.L., 1982b, ApJ, 261, 595
- Danziger, I.J. 1963, Ph.D. dissertation, Australian National University
- Feast, M.W., Carter, B.S., Roberts, G., Marang, F., Catchpole, R.M. 1997, MNRAS, 283, 317
- Giridhar, S., Lambert, D.L., Reddy, B.E., Yong, D. 2005, ApJ, 627, 432
- Gonzalez, G., Lambert, D.L., Wallerstein, G., Rao, N.K., Smith, V.V., McCarthy, J.M. 1998, ApJS, 114, 133
- Herbig, G.H. 1949, ApJ, 110, 143
- Jeffery, C.S., Heber, U. 1993, A&A, 270, 167
- Lambert, D. L., Rao, N. K., 1994, JAA, 15, 47
- Lambert, D. L., Rao, N. K., Pandey G., Ivans, I., 2001, ApJ, 555, 925
- Lawson, W. A., Cottrell, P.L. 1997, MNRAS, 285, 266
- Lawson, W. A., Cottrell, P. L., Clark, M., 1991, MNRAS, 251, 687
- Lodders, K. 2003, ApJ, 591, 1220
- Pandey, G., Lambert, D.L., Jeffery, C.S., Rao, N.K. 2006, ApJ, 638, 454
- Pandey, G., Rao, N.K., Lambert, D.L., Jeffery, C.S. 2001, MNRAS, 324, 937
- Pandey, G., Reddy, B.E. 2006, MNRAS, 369, 1677
- Payne-Gaposchkin, C. 1963, ApJ, 138, 320
- Percy, J.R., Bandara, K., Cottrell, P. L., Skuljan, L. 2004, JAVSO, 33, 27
- Rao N.K. 2005, in Barnes, T.G., Bash, F.N., eds., Cosmic Abundances as Records of Stellar Evolution and Nucleosynthesis, ASPC, 336, 185
- Rao N.K., Lambert D.L., 2000, MNRAS, 313, L33
- Rao N.K., Lambert D.L., 2003, PASP, 115, 1304
- Rao N.K., Lambert D.L., Adams, M.T., Doss, D.R., Gonzalez, G., Hatzes, A.P., James, R., Johns-Krull, C.M., Luck, R.E., Pandey, G., Reinsch, K., Tomkin, J., Woolf, V.M. 1999, MNRAS, 310, 717
- Rao, N.K., Lambert, D.L., Shetrone, M.D. 2006, MNRAS, 370, 941
- Saio, H., Jeffery, C.S. 2002, MNRAS, 333, 1210
- Schwarz, G.J., Shore, S.N., Starrfield, S., Vanlandingham, K.M. 2007, ApJ, 657, 453
- Skuljan, L., & Cottrell, P.L. 2002, Obs., 122, 322
- Skuljan, L., & Cottrell, P.L., 2004, in Kurtz, D.W., Pollard, K.R., eds., Variable Stars in the Local Group, ASPC, 310, 511
- Spitzer, L. Jr. 1968, Diffuse Matter in Space, Interscience Publications, New York
- Tenenbaum, E.D., Clayton, G.C., Asplund, M., Engelbracht, C.W., Gordon, K.D., Hanson, M.M., Rudy, R.J., Lynch, D.K., Mazuk, S., Venturini, C.C., Puetter, R.C. 2005, A&A, 430, 256
- Tull, R.G., MacQueen, P.J., Sneden, C., Lambert, D.L., 1995, PASP, 107, 251
- Warner, B., 1967, MNRAS, 137, 119
- Whitney, B.A., Clayton, G.C., Schulte-Ladbeck, R.E., Mead, M.R. 1992, AJ, 103, 1652
- Woitke, P. 2006, A&A, 452, 537
- Woitke, P., & Niccolini, G. 2005, A&A, 433, 1101
- Woitke, P., Goeres, A., Sedlmayr, E., 1996, A&A, 313, 217